Inorganica Chimica Acta 363 (2010) 2637–2642

Contents lists available at ScienceDirect

Inorganica Chimica Acta

journal homepage: www.elsevier.com/locate/ica

Observation of a mixed-metal transition in a d^8–d^{10} heterobimetallic Pt–Ag cyanide system: Experimental and theoretical study

François Baril-Robert [a], Veladri Palla [a], Xiaobo Li [a], Renante Yson [b], Howard H. Patterson [a,*]

[a] Department of Chemistry, University of Maine, Orono, Maine 04469-5706, United States
[b] Department of Chemistry, University of Nevada, Reno, Nevada 89557, United States

ARTICLE INFO

Article history:
Received 12 March 2010
Accepted 3 May 2010
Available online 11 May 2010

Keywords:
Mixed-metal compounds
Luminescence
DFT
MLCT
Closed shell ions

ABSTRACT

Photoluminescence spectra of synthesized crystals of the mixed-metal heterobimetallic $Ba\{[Ag(CN)_2]_{2-2x}[Pt(CN)_4]_x\}$ ($x = 0 \rightarrow 1$) were recorded at 300, 150 and 77 K. Emission of the mixed-metal system containing both $[Pt(CN)_4]^{2-}$ and $[Ag(CN)_2]^-$ ions shows an emission band due to Pt–Ag interaction. This new peak (424 nm) is not seen for pure $Ba[Pt(CN)_4]$ or $Ba[Ag(CN)_2]_2$. Theoretical DFT and extended Hückel molecular orbital population calculations shows that in heterometallic dimers, the HOMO correspond to d_z2 of the metals with a weakly antibonding interaction between the moieties while the LUMO π^*(CN) orbital shows a stronger bonding character between monomers. This indicate that the 424 nm emission peak corresponds to a MLCT ($d \rightarrow \pi^*$) transition with some metal to metal charge transfer character (Pt to Ag).

1. Introduction

Photochemistry of closed shell d^8 and d^{10} complexes has attracted a great deal of attention over the past few years [1–9]. These cyanide complexes exhibit relatively strong emission bands assigned to a transition from a metal HOMO orbital to a π^*(CN) LUMO [10,11]. The strong oscillator strength of the spin and Laporte allowed MLCT transitions allows spectroscopic study on low concentration samples (diluted solutions or doped compounds) and have potentially room temperature photophysical and photochemical applications such as volatile organic compounds detection [12,13], ion sensors [14,15], oxygen sensors [16], molecular light-emitting devices [17–19] and photoassisted degradation of pollutants [20].

Square-planar and linear configurations (d^8 and d^{10} systems, respectively) open the possibility for interactions between coordinatively unsaturated metal ions. It has been shown that d^8–d^8 and d^{10}–d^{10} metallophilic interactions can be relatively strong (~10 kcal/mol) [21] with the formation of exciplexes and extended polymers [22]. Compared to the monomeric species, metal–metal bonded oligomers exhibit a red-shift of their first excited state. This phenomena gives the concentration, temperature and excitation wavelength tunability observed for several compounds [6–9]. For example, our group has reported excimer and exciplex formation for silver dicyanide anions doped in alkali halide lattices with tuning over 18,000 cm^{-1} by site-selective excitation of each $[Ag(CN)_2]^-$ nanocluster [8,9].

There are numerous examples of Ag(I) coordination compounds with short Ag–Ag internuclear separations that have been structurally characterized, ranging from dimers to infinite chains or clusters. In most of these silver compounds, the Ag–Ag interactions are assisted by the presence of bridging or capping ligands. Very few examples of ligand unsupported Ag(I) aggregates have been reported [6,23–26]. We have reported the crystal structure, electronic structure and temperature dependent Raman spectra of $Tl[Ag(CN)_2]$ as an example of ligand unsupported argentophilic interactions. The photoluminescence temperature dependent spectra of single crystals of $Tl[Ag(CN)_2]$ showed several photophysical properties consistent with exciplex emission. *Ab initio* and extended Hückel calculations indicate exciplex formation with a deep potential well in the lowest-excited electronic state.

The platinum tetracyanide −2 ion is another ion studied for its potential metallophilic interactions occurring along the axial orientation. This structural feature has triggered research on unidimensional electric conductivity of such materials [27]. Similarly to the silver dicyanide compounds, the metal–metal separation influence the HOMO and LUMO energy. This is nicely shown by the crystallographic and spectroscopic studies done on two forms of erbium tetracyanoplatinate [28]. The first form has a relatively short platinum–platinum distance (~3.17 Å) and luminesces at low energy (~16,000 cm^{-1}) while the second form has longer Pt–Pt bonds (3.27–3.40 Å) and emits at higher energy (~19,500 cm^{-1}). It is known that a relationship between the electronic

---

* Corresponding author. Fax: +1 207 581 1191.
E-mail address: howardp@maine.edu (H.H. Patterson).

0020-1693/$ - see front matter © 2010 Elsevier B.V. All rights reserved.
doi:10.1016/j.ica.2010.05.001

structure and the metal–metal separation exists in these platinum cyanide systems [28].

Mixtures of two d^8 and/or d^{10} cyanide compounds of different metals are less known [29–31]. The M–M distance and electronic structure correlation is less predictable. In addition, the nature of the metal centers, the mixture ratios and the different constitutional isomers may have important effects on the energy and character of the frontier orbitals. When $La[Ag_xAu_{1-x}(CN)_2]_3$ crystals were studied using both steady-state and time-resolved luminescent methods [32], the mixed Ag–Au crystals display an anomalously strong luminescence at ambient temperatures that is tunable by changing temperature, excitation wavelength and Ag/Au ratio. Also, crystals of the $K[Au_xAg_{1-x}(CN)_2]$ mixed-metal system have been studied [33]. In this case, a new emission band is observed for this mixed-metal system which is not seen in pure $K[Ag(CN)_2]$ or pure $K[Au(CN)_2]$ crystals. Extended Hückel calculations indicate the formation of excimers with the luminescence assigned to a mixed-metal transition from a molecular orbital with Au character to a molecular orbital with Ag character. Another mixed-metal system studied is the $Ba[Pt_xM_{1-x}(CN)_4]$ (M = Pd or Ni) [34]. Tunability of the delocalized electronic states is observed in the palladium doped material while the platinum/nickel mixture exhibits energy transfer from a delocalized platinum–nickel excited electronic state to platinum tetracyanide clusters.

In light of these d^8 or d^{10} system results, it is important to ask what factors determine the presence, energy and intensity of mixed-metal transitions. To probe these factor, we report in this paper, a theoretical and experimental study of the mixed d^{10}–d^8 system $Ba\{[Ag(CN)_2]_{2-2x}[Pt(CN)_4]_x\}$ ($x = 0$, 0.40, 0.86 and 1). In this study reported herein, a simple mixed-metal system with only cyanide ligands should allow us to probe important structural and electronic features controlling the photophysical behavior of such compounds.

2. Experimental

The synthesis of pure crystals of $Ba[Pt(CN)_4]$ and $Ba[Ag(CN)_2]_2$ was accomplished by slow diffusion of methanol vapor in an aqueous solution containing the proper stoichiometric amounts of $Ba(NO_3)_2$ with $K[Ag(CN)_2]$ or $K_2[Pt(CN)_4]$. Pure crystals in each case were harvested in about 5 days. A similar procedure, using these three salts, was used to obtain the mixed-metal materials $Ba\{[Ag(CN)_2]_{2-2x}[Pt(CN)_4]_x\}$ with $x = 0.40$ (Pt:Ag 1:3) and 0.86 (Pt:Ag 3:1). All of the chemicals used were purchased from Alfa-Aesar in at least 99.5% purity.

Emission and excitation spectra were collected using a Photon Technology International Model QuantaMaster-1046 spectrophotometer. This instrument is equipped with a 75W xenon lamp, two excitation monochromators, an emission monochromator, and a detector. Emission and excitation spectra were recorded at different temperatures of 78, 150 and room temperature. Initially a single crystal of one of the samples was mounted on a copper holder and cooled down to the desired temperature and emission and excitation spectra were recorded after 30 min.

Extended Hückel calculations were carried out for the ground and first excited states of the $[Ag(CN)_2]^-$ dimer, $[Pt(CN)_4]^{2-}$ dimer and the $\{[Ag(CN)_2][Pt(CN)_4]\}^{3-}$ dimer as well as $\{[Ag(CN)_2][Pt(CN)_4][Ag(CN)_2]\}^{4-}$ and $\{[Pt(CN)_4][Ag(CN)_2][Pt(CN)_4]\}^{5-}$ trimers with direct Pt–Ag overlap in the z-direction. Bond distances and dihedral angles for $[Ag(CN)_2]^-$ and $[Pt(CN)_4]^{2-}$ were optimized. Potential energy diagrams of the ground and first excited states were generated by calculating the energy of each dimer as the metal–metal separation is varied. The program ICON-EDIT [35] was used for the extended Hückel calculations.

The theoretical structure of the $[Pt(CN)_4]^{2-}$ (D_{4d} square planar) and $[Ag(CN)_2]^-$ ($D_{\infty h}$ linear) were optimized using the GAUSSIAN '03 (Gaussian Inc.) [36] software. These theoretical structures and the metal–metal bond length derived from the extended Hückel calculations were used to create the different dimer and trimer models. The density functional theory calculations were performed using the B3LYP functional [37–39] and the SDD basis set [40,41] as implemented in the software. Excited state energies were calculated using the time-dependent theory (TD-DFT) [42–44]. Counterpoise correction for basis set superposition error [45,46] was used to determine the interaction between two moieties of the different dimers. The GAUSSVIEW 3.0 program [47] allowed us to visualize the isodensity contour maps of the different orbitals. The *ab initio* calculations were performed on the University of Maine supercomputer.

3. Results and discussion

3.1. Spectroscopic study

Spectroscopy of d^8 and d^{10} cyanide compounds is governed by MLCT (d_z2 to π^*) transitions. The 77 K emission spectra ($\lambda_{ex} = 330$ nm) of $Ba[Ag(CN)_2]_2$, $Ba[Pt(CN)_4]$ and $Ba\{[Ag(CN)_2]_{2-2x}[Pt(CN)_4]_x\}$ (where $x = 0.40$ and 0.86) materials are shown in Fig. 1. The cases of $x = 0.40$, 0.86 corresponds to a stoichiometric ratio of Ag to Pt of 3:1 and 1:3, respectively. The $Ba[Ag(CN)_2]_2$ spectra exhibits a single emission maximum at 409 nm while $Ba[Pt(CN)_4]$ shows two peaks at 410 nm and 458 nm. These two emission peaks have similar excitation spectra (*vide infra*) and are considered to be MLCT spin allowed and spin forbidden transitions. The mixed-metal crystals show peaks at 424 nm and a shoulder at ~460 nm. Due to the platinum content dependency of this shoulder's relative intensity and to the emission and excitation energies, this 460 nm was assigned to barium platinum tetracyanide co-crystallized impurities. The new peak at 424 nm seen in the case of the barium mixed-metal crystals, and not in the case of pure $Ba[Ag(CN)_2]_2$ and $Ba[Pt(CN)_4]$, is assigned to an emission from a mixed-metal species. The band maximum of this transition is situated between the low energy emission of the $Ba[Pt(CN)_4]$ compound (458 nm) and the higher energy emission of the $Ba[Ag(CN)_2]_2$ complex (409 nm). Variation in the silver to platinum ratio does not significantly change the energy of the mixed-metal transition, suggesting the presence of a single type of mixed-metal cluster in the two compounds studied.

The low temperature (77 K) excitation spectra corresponding to the emission peaks of $Ba[Ag(CN)_2]_2$, $Ba[Pt(CN)_4]$ and $Ba\{[Ag$

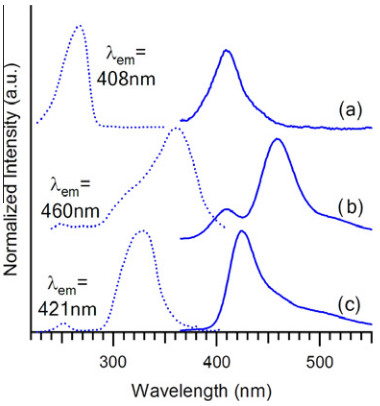

Fig. 1. Excitation and emission ($\lambda_{ex} = 330$ nm) spectra of (a) $Ba[Ag(CN)_2]_2$, (b) $Ba[Pt(CN)_4]$ and (c) $Ba\{[Ag(CN)_2]_{1.20}[Pt(CN)_4]_{0.40}\}$ at 77 K. Emission wavelength used for the acquisition of the excitation spectra are indicated on the corresponding spectra.